Quaternary Geochronology 30 (2015) 1–8

Contents lists available at ScienceDirect

Quaternary Geochronology

journal homepage: www.elsevier.com/locate/quageo

Research paper

The mathematical basis for the US-ESR dating method

Qingfeng Shao [a,*], John Chadam [b], Rainer Grün [c], Christophe Falguères [d], Jean-Michel Dolo [e], Jean-Jacques Bahain [d]

[a] College of Geography Science, Nanjing Normal University, 1, Wenyuan Road, 210023 Nanjing, China
[b] Department of Mathematics, University of Pittsburgh, Pittsburgh, PA 15260, USA
[c] Research School of Earth Sciences, The Australian National University, ACT 0200 Canberra, Australia
[d] Département de Préhistoire, Muséum National d'Histoire Naturelle, UMR7194, 1, Rue René Panhard, 75013 Paris, France
[e] CEA, I[2]BM, 91401 Orsay Cedex, France

ARTICLE INFO

Article history:
Received 20 January 2015
Received in revised form
15 July 2015
Accepted 28 July 2015
Available online 1 August 2015

Keywords:
ESR/U-series dating method
US-ESR model
U-uptake
Dose rate evolution
Fossil teeth

ABSTRACT

Over the past two decades, the combined electron spin resonance (ESR) and U-series dating method has been widely applied to date fossil teeth for archaeological studies through the use of the US-ESR model. The obtained age, compatible with both the ESR and U-series data determined in all dental tissues and the burial environment, is more flexible and reliable than the parametric uptake ages (by early, linear or recent uptake models), for which selection was often based on the expected age of the site. In this paper, the mathematical basis of the US-ESR model is described in detail, from the U-uptake description to the calculation of accumulation dose in the sample and the US-ESR age determination. An example is used to illustrate the calculation of the US-ESR age, associated dose rates and U-uptake parameters. While the description in this paper is specific to US-ESR model and more largely combined ESR/U-series dating of fossil teeth, we expect that some of the principles can be used in other applications of U-series dating.

1. Introduction

Grün et al. (1988) proposed a U-uptake model for ESR dating of fossil teeth based on a smooth diffusion function: $U_8(t) = U_{8m}(t/T)^{p+1}$, where $U_8(t)$ is the ^{238}U concentration at a time t in a dental tissue, U_{8m} the measured, present day ^{238}U concentration, T the apparent age of the tooth and p the U-uptake parameter ($-1 \leq p < \infty$).

In this model, ESR dose rate evaluations are derived from measured U-series disequilibria between ^{238}U, ^{234}U and ^{230}Th in all dental tissues (enamel, dentine and cement) contributing to the irradiation of the tooth enamel. This dating approach is often called combined ESR/U-series dating and yields US-ESR age estimates.

Over the past two decades, the combined ESR/U-series dating approach has become a commonly used geochronological tool and has produced hundreds of age estimates for archaeological sites. In this paper, we describe the mathematical basis of this dating model. While the description in this paper is specific to combined ESR/U-series dating of fossil teeth, we expect that some of the principles can be used in other applications of U-series dating.

2. Mathematical model

The US model is based on four assumptions (Grün et al., 1988):

1) there are no U-series nuclides in the dental tissues before burial (i.e., $U(t) = 0$ for $t = 0$);
2) the ^{234}U/^{238}U activity ratio (r_0) in the burial environment is constant over time;
3) there is no Th uptake;
4) there is no net loss of any of the isotopes at any time.

For the equations that follow, it is convenient to define the following parameters:

p: U-uptake parameter,
T: age of the sample,
U_{8m}: measured, present day ^{238}U concentration in dental tissues,
U_8, U_4, U_0: concentrations of ^{238}U, ^{234}U and ^{230}Th,
λ_8, λ_4, λ_0: decay constants of ^{238}U, ^{234}U and ^{230}Th (e.g., Cheng et al., 2013),

* Corresponding author.
E-mail addresses: 09396@njnu.edu.cn (Q. Shao), chadam@pitt.edu (J. Chadam), rainer.grun@anu.edu.au (R. Grün), falguere@mnhn.fr (C. Falguères), jean-michel.dolo@cea.fr (J.-M. Dolo), bahain@mnhn.fr (J.-J. Bahain).

http://dx.doi.org/10.1016/j.quageo.2015.07.002
1871-1014/

R_{48}, R_{08}: $^{234}U/^{238}U$ and $^{230}Th/^{238}U$ activity ratios,
r_0: $^{234}U/^{238}U$ activity ratio in the burial environment,
S_8, S_4: concentrations of ^{238}U and ^{234}U diffusing into the dental tissues per unit time.

With this model, the dynamics of the three U-series nuclides of interest, ^{238}U, ^{234}U and ^{230}Th, in the dental tissues are described as follows:

$$\frac{dU_8(t)}{dt} = S_8(t) - \lambda_8 U_8(t) \tag{1}$$

$$\frac{dU_4(t)}{dt} = S_4(t) - \lambda_4 U_4(t) + \lambda_8 U_8(t) \tag{2}$$

$$\frac{dU_0(t)}{dt} = \lambda_4 U_4(t) - \lambda_0 U_0(t). \tag{3}$$

Each of these differential equations is of the form:

$$\frac{dy}{dt} = Ay + B(t) \tag{4}$$

and has a unique solution:

$$y(t) = y(t_0)e^{A(t-t_0)} + \int_{t_0}^{t} e^{A(t-\tau)}B(\tau)d\tau. \tag{5}$$

Using the initial condition of $U_8(t_0) = U_4(t_0) = U_0(t_0) = 0$ (with $t_0 = 0$), the concentrations of ^{238}U, ^{234}U and ^{230} Th at a given time are:

$$U_8(t) = \int_0^t S_8(\tau)e^{-\lambda_8(t-\tau)}d\tau \tag{6}$$

$$U_4(t) = \int_0^t [\lambda_8 U_8(\tau) + S_4(\tau)]e^{-\lambda_4(t-\tau)}d\tau \tag{7}$$

$$U_0(t) = \int_0^t \lambda_4 U_4(\tau)e^{-\lambda_0(t-\tau)}d\tau. \tag{8}$$

If ^{238}U concentration diffusing into a dental tissue is expressed as $S_8(t) = ct^p$, it follows from Eq. (6):

$$U_8(t) = c\int_0^t \tau^p e^{-\lambda_8(t-\tau)}d\tau \cong c\int_0^t \tau^p d\tau = \frac{ct^{p+1}}{p+1} \tag{9}$$

using the fact that $exp-(-\lambda_8(t-\tau)) \approx 1$, because $\lambda_8(t-\tau) < \lambda_8 T \approx 1.551 \times 10^{-5}$ is much less than $\lambda_4 T \approx 0.282$ or $\lambda_0 T \approx 0.917$ for the ages $T \geq 10^5$ years.

The measured value of ^{238}U at T, $U_{8m} = U_8(T) = cT^{(p+1)}/(p+1)$, implies that $c = (p+1)U_{8m}/T^{(p+1)}$, resulting in:

$$S_8(t) = (p+1)\frac{U_{8m}}{T^{p+1}}t^p. \tag{10}$$

Combining this with Assumption 2 results in:

$$S_4(t) = r_0\frac{\lambda_8 S_8(t)}{\lambda_4} = r_0\frac{\lambda_8(p+1)U_{8m}t^p}{\lambda_4 T^{p+1}}. \tag{11}$$

Using (9)–(11) in the solutions (6)–(8) and introducing $s = \tau/t$ (see Appendix 1) yields:

$$U_8(t) = U_{8m}(t/T)^{p+1} \tag{12}$$

$$U_4(t) = \frac{\lambda_8 U_8(t)}{\lambda_4}\left[r_0 - \lambda_4 t(r_0 - 1)\int_0^1 s^{p+1}e^{-\lambda_4 t(1-s)}ds\right] \tag{13}$$

$$U_0(t) = \frac{\lambda_8 U_8(t)}{\lambda_0 - \lambda_4}\left[t(r_0\lambda_0 - \lambda_4)\int_0^1 s^{p+1}e^{-\lambda_0 t(1-s)}ds - \lambda_4 t(r_0 - 1)\int_0^1 s^{p+1}e^{-\lambda_4 t(1-s)}ds\right]. \tag{14}$$

3. Relationship between *p* and *T*

Using Eqs. (12)–(14), the $^{234}U/^{238}U$ and $^{230}Th/^{238}U$ activity ratios at the putative age, T, of the sample can be expressed as:

$$R_{48}(T) = \frac{\lambda_4 U_4(T)}{\lambda_8 U_8(T)} = r_0 - \lambda_4 T(r_0 - 1)\int_0^1 s^{p+1}e^{-\lambda_4 T(1-s)}ds \tag{15}$$

$$R_{08}(T) = \frac{\lambda_0 U_0(T)}{\lambda_8 U_8(T)} = \frac{\lambda_0}{\lambda_0 - \lambda_4}\left[T(r_0\lambda_0 - \lambda_4)\int_0^1 s^{p+1}e^{-\lambda_0 T(1-s)}ds - \lambda_4 T(r_0 - 1)\int_0^1 s^{p+1}e^{-\lambda_4 T(1-s)}ds\right]. \tag{16}$$

Inserting the measured values of the activity ratios for $R_{48}(T)$ and $R_{08}(T)$ and solving Eqs. (15) and (16) for r_0 (see Appendix 2) results in:

$$r_0 = \frac{R_{48} - \lambda_4 T\int_0^1 s^{p+1}e^{-\lambda_4 T(1-s)}ds}{1 - \lambda_4 T\int_0^1 s^{p+1}e^{-\lambda_4 T(1-s)}ds} \tag{17}$$

and

$$r_0 = \frac{R_{48} - \left(\frac{\lambda_0 - \lambda_4}{\lambda_0}\right)R_{08} - \lambda_4 T\int_0^1 s^{p+1}e^{-\lambda_0 T(1-s)}ds}{1 - \lambda_0 T\int_0^1 s^{p+1}e^{-\lambda_0 T(1-s)}ds}. \tag{18}$$

Eliminating r_0 by combination of Eqs. (17) and (18) gives the p–T relationship in the form of (see Appendix 2):

$$a_4 y(p, cx) - [a_4 - (1-c)a_0]y(p, x) + (1-c) = 0 \tag{19}$$

where $x = \lambda_0 T$, $c = \lambda_4/\lambda_0$, $a_4 = R_{48} - 1$ and $a_0 = R_{08} - 1$ with

$$y(p, x) = \left[1 - x\int_0^1 s^{p+1}e^{-x(1-s)}ds\right]^{-1}. \tag{20}$$

The above equations provide the relationship between p and T

derived for experimentally measured values of the activity ratios.

4. Dose accumulation

The US-ESR procedure for determining the age relies on using the measured value of the total dose obtained by ESR analysis on tooth enamel to provide a second equation in p and T.

In the following section, we will use the following notations:

a_β^8, a_β^0: beta attenuation factors for ^{238}U– ^{234}U and ^{230}Th– ^{206}Pb (Marsh, 1999),
b_β^8, b_β^0: beta self absorption factors for β-dose rates ^{238}U–^{234}U and ^{230}Th– ^{206}Pb (Marsh, 1999),
d_α^8, d_α^4, d_α^0: alpha dose rates for ^{238}U–^{234}U, ^{234}U– ^{230}Th and ^{230}Th– ^{206}Pb (Guérin et al., 2011),
d_β^8, d_β^0: beta dose rates for ^{238}U–^{234}U and ^{230}Th– ^{206}Pb (Guérin et al., 2011),
f_W^α, f_W^β: α, β water attenuation factors (Grün, 1994),
k: alpha efficiency (Grün and Katzenberger-Apel, 1994),
C_8, C_4, C_0: total dose rates for ^{238}U–^{234}U, ^{234}U– ^{230}Th and ^{230}Th– ^{206}Pb, the latter can be adjusted for ^{222}Rn loss (Guérin et al., 2011),
C_U, C_{Th}, C_k: total dose rates from U, Th and K (Guérin et al., 2011),
D_{ena}, D_{den}, D_{cem}, D_{env}: total dose contributed by enamel, dentine, cement and environment (mainly sediments and cosmic rays) from the radioactive isotopes in enamel, dentine, cement and the environment.
D_e: dose value measured by ESR analysis in enamel, $D_e = D_{ena} + D_{den} + D_{cem} + D_{env}$.

4.1. Internal dose, $D_{ena}(T, p)$

The internal dose, D_{ena}, is generated by α and β-particles emitted from the U incorporated into enamel and its daughter isotopes. The accumulated internal dose from the time the tooth was formed ($t = 0$) to today ($t = T$) can be expressed by:

$$D_{ena}(T,p) = \int_0^T \left[C_8 U_8(t) + \frac{\lambda_4}{\lambda_8} C_4 U_4(t) + \frac{\lambda_0}{\lambda_8} C_0 U_0(t)\right] dt. \quad (21)$$

The corresponding dose rate of C_8 is:

$$C_8 = \frac{k}{f_W^\alpha} d_\alpha^8 + \frac{1}{f_W^\beta} b_\beta^8 d_\beta^8. \quad (22)$$

The dose rates of C_4 and C_0 are in the similar form.

Inserting Eqs. (12)–(14) into (21) and introducing $u = t/T$ allows the calculation of $D_{ena}(T, p)$ as follows (see details of calculation in Appendix 3):

$$D_{ena}(T,p) = \frac{U_{8m}T(C_8 + C_4 r_0)}{p+2} - C_4 U_{8m} \lambda_4 T^2 (r_0 - 1) \int_0^1 \int_0^1 u^{p+2} s^{p+1} e^{-\lambda_4 uT(1-s)} duds + \frac{\lambda_0}{\lambda_0 - \lambda_4} C_0 U_{8m} T^2 \left[(r_0\lambda_0 - \lambda_4) \int_0^1 \int_0^1 u^{p+2} s^{p+1} e^{-\lambda_0 uT(1-s)} duds - \lambda_4 (r_0 - 1) \int_0^1 \int_0^1 u^{p+2} s^{p+1} e^{-\lambda_4 uT(1-s)} duds \right] \quad (23)$$

where r_0 is obtained from Eq. (17) or (18).

4.2. External dose from dentine, $D_{den}(T, p)$

The dentine dose is generated by β-particles from the U incorporated into the dentine and its daughter isotopes. Enamel sample preparation usually involves the removal of the outer 50 μm, which eliminates the volume that received irradiation by external α-particles. The γ-dose from dentine is also considered to be negligible because γ-rays have long effective ranges (>20 cm) compared with enamel thickness (0.1–0.2 cm). However, for larger teeth (e.g., elephants or mammoths) the gamma dose rate generated within the tooth may contribute significantly to the enamel dose rate (Nathan and Grün, 2003).

The integrated dentine β-dose in the enamel from 0 to T can be expressed as:

$$D_{den}(T,p) = \int_0^T \left[C_8' U_8(t) + \frac{\lambda_0}{\lambda_8} C_0' U_0(t)\right] dt. \quad (24)$$

Note that the decay from ^{234}U to ^{230}Th does not involve β-emissions. Following the same approach, C_8', the total dose rate for ^{238}U–^{234}U in dentine and cement, is given by:

$$C_8' = \frac{1}{f_W^\beta} f_\beta^8 a_\beta^8 d_\beta^8. \quad (25)$$

C_0', the total dose rate for ^{230}Th to ^{206}Pb in dentine and cement, is in the similar form.

Introducing $U_8(t)$ and $U_0(t)$ from Eqs. (12) and (14) into the previous equation and following the same type of calculations as in Appendix 3, yields:

$$D_{den}(T,p) = \frac{C_8' T U_{8m}}{p+2} + \frac{\lambda_0}{\lambda_0 - \lambda_4} C_0' U_{8m} T^2 \left[(r_0\lambda_0 - \lambda_4) \int_0^1 \int_0^1 u^{p+2} s^{p+1} e^{-\lambda_0 uT(1-s)} duds - \lambda_4 (r_0 - 1) \int_0^1 \int_0^1 u^{p+2} s^{p+1} e^{-\lambda_4 uT(1-s)} duds \right]. \quad (26)$$

4.3. External dose from cement, $D_{cem}(T, p)$

The expressions of external dose from dentine, Eqs. (24)–(26), are also applicable to cement, if it covers one side of the enamel surface. Hence, the $D_{cem}(T, p)$ is:

$$D_{cem}(T,p) = \frac{C_8' T U_{8m}}{p+2} + \frac{\lambda_0}{\lambda_0 - \lambda_4} C_0' U_{8m} T^2 \left[(r_0\lambda_0 - \lambda_4) \int_0^1 \int_0^1 u^{p+2} s^{p+1} e^{-\lambda_0 uT(1-s)} duds - \lambda_4 (r_0 - 1) \int_0^1 \int_0^1 u^{p+2} s^{p+1} e^{-\lambda_4 uT(1-s)} duds \right]. \quad (27)$$

4.4. External dose from environment, $D_{env}(T)$

The dose from the environment into the enamel is defined here as the sum of β (if the enamel is not shielded by cement) and γ-doses generated by U, Th and K from burial environment (mainly sediments) and the dose generated by cosmic rays, over a time from 0 to T:

$$D_{env}(T) = D_U(T) + D_{Th}(T) + D_K(T) + D_{cos}(T). \quad (28)$$

If the U and Th decay chains are in secular equilibrium state, the calculations are straightforward. Note that the external gamma dose rate is usually measured in situ rather than derived from the analysis of a sediment sample. The calculations of the beta and gamma dose rates involve beta attenuation factors and corrections for water contents (see above). The cosmic rays have to be corrected for sediment shielding (Prescott and Hutton, 1994). Finally, the total dose is given by:

$$D_e(T,p) = D_{ena}(T,p) + D_{den}(T,p) + D_{cem}(T,p) + D_{env}(T). \quad (29)$$

5. US-ESR age determination

The estimated age, T_e, is then obtained from the measured data R_{48}, R_{08} and D_e with the following procedure:

Step 1 – Take an increasing sequence of values of $p_i < p_{i+1}$ and use the measured values of R_{48} and R_{08} to calculate the corresponding increasing sequence of values of $x_i(=\lambda_0 T_i)$ using Eq. (19), in order to establish the p–T relationship for each dental tissue.

Step 2 – Use these values from step 1 in Eq. (17) or (18) for r_0 and in Eq. (29) to calculate the dose components ($D_{ena}(T, p)$, $D_{dent}(T, p)$, $D_{cem}(T, p)$). The single and double integrals that appear can be numerically calculated using commercial software packages (e.g., *Matlab*©, see Appendix 4). This provides the model's estimate D_i of the total dose for the uptake parameter, p_i. Continue this procedure to identify values $p_i < p_{i+1}$ which provide sufficiently tight bounds of the form:

$$D_i < D_e < D_{i+1}. \quad (30)$$

Step 3 – The final step is to use the method of bisection to find the value of p_e, and the corresponding $x_e(=\lambda_0 T_e)$ for which $D(p_e, T_e) = D_e$.

In applications of dating fossil teeth, the US-ESR age calculation can be performed either on the DATA program (Grün, 2009) or the USESR program (Shao et al., 2014).

6. Example of US-ESR age calculation

To illustrate the age determination, the data of Table 1 (also used in Shao et al., 2014) were used to calculate a US-ESR age estimate and the associated parameters.

The first step is to calculate the p–T relationship for each dental tissue. For the enamel, taking the measured activity ratios, $R_{48} = 1.37$ and $R_{04} = 0.81$, and using the decay rates of $\lambda_4 = 2.82 \times 10^{-6}\ \text{a}^{-1}$ and $\lambda_0 = 9.17 \times 10^{-6}\ \text{a}^{-1}$, one has $c = \lambda_4/\lambda_0 = 0.308$, $a_4 = 0.37$, $a_0 = 0.1097$. Thus Eq. (19) becomes, for $y(p, x)$ given by Eq. (20),

$$0.37y(p, 0.308x) - 0.294y(p,x) + 0.692 = 0. \quad (31)$$

For each $p \geq 1$ one can numerically solve Eq. (20) for x (see Appendix 4) and plotting the results one obtains the p–T relationship (Fig. 1A). In spite of the complicated functional form of Eq. (20), its graph is very nearly a straight line (see Appendix 4).

With the calculated p–T relationship, the data of Table 1 can be inserted into Eqs. (21)–(28) to calculate the dose components, $D_{ena}(T, p)$, $D_{den}(T, p)$, $D_{cem}(T, p)$, $D_{env}(T)$ (Fig. 1B). The γ-dose from the external environment was assumed to be constant over time. The sum of each component yields the paleodose, D_i (Fig. 1C).

Finally, comparing the measured D_e value (1196 ± 60 Gy) with the calculated D_i, the age estimate (726 + 87/−84 ka) can be determined (Fig. 1C). Then, one can derive the time averaged internal dose rate (444 ± 147 μGy/a), dentine β-dose rate (222 ± 66 μGy/a), cement β-dose rate (149 ± 43 μGy/a) and total dose rate (1647 ± 177 μGy/a) (Fig. 1B). Using the age estimate and the calculated p–T relationships, p-values (0.50 ± 0.33, 0.32 ± 0.28 and 0.33 ± 0.27) for enamel, dentine and cement, respectively, are readily determined (Fig. 1A).

7. Conclusions

This paper presents the mathematical basis of the US-ESR dating model. This model has been successfully applied at numerous sites and provides a major advance over the parametric early, linear or recent uptake ages, whose selection was often based on the expected age of the site. With laser ablation we are now able to measure the spatial distribution of U concentrations and U-series isotopes. Initial results indicate that U-uptake is a fast process (Grün et al., 2014), i.e., the CSUS-ESR model may be more appropriate for such samples (Grün, 2000). It may seem timely to develop a model that accounts for measured spatial distributions of U-series isotopes. Until then we strongly advise using the measured ESR and U-series data for the calculation of both US-ESR and CSUS-ESR age estimates. The range provided by these age estimates encompasses all continuous U-uptake histories, and is thus independent of the

Table 1
The data used as an example for US-ESR age calculation.

Parameter	Material	Value	Error
D_e (Gy)	Enamel	1196	60
U (ppm)	Enamel	2.85	0.23
$^{234}U/^{238}U$	Enamel	1.37	0.03
$^{230}Th/^{234}U$	Enamel	0.81	0.02
$^{210}Pb/^{230}Th$	Enamel	0.65	0.10
Water (wgt%)	Enamel	0	0
U (ppm)	Dentine	68.00	4.08
$^{234}U/^{238}U$	Dentine	1.36	0.03
$^{230}Th/^{234}U$	Dentine	0.83	0.03
$^{210}Pb/^{230}Th$	Dentine	0.35	0.08
Water (wgt%)	Dentine	7	1
U (ppm)	Cement	48.44	2.91
$^{234}U/^{238}U$	Cement	1.37	0.03
$^{230}Th/^{234}U$	Cement	0.83	0.03
$^{210}Pb/^{230}Th$	Cement	0.29	0.08
Water (wgt%)	Cement	7	2
Total thickness (μm)	Enamel	1389	167
Removed side 1 (μm)	Enamel	127	20
Removed side 2 (μm)	Enamel	126	20
U (ppm)	Sediment	3.0	0.2
Th (ppm)	Sediment	7.0	0.4
K (%)	Sediment	0.98	0.03
Water (wgt%)	Sediment	13	3
Cosmic dose rate (μGy/a)		0	0
In situ dose rate (μGy/a)		832	58

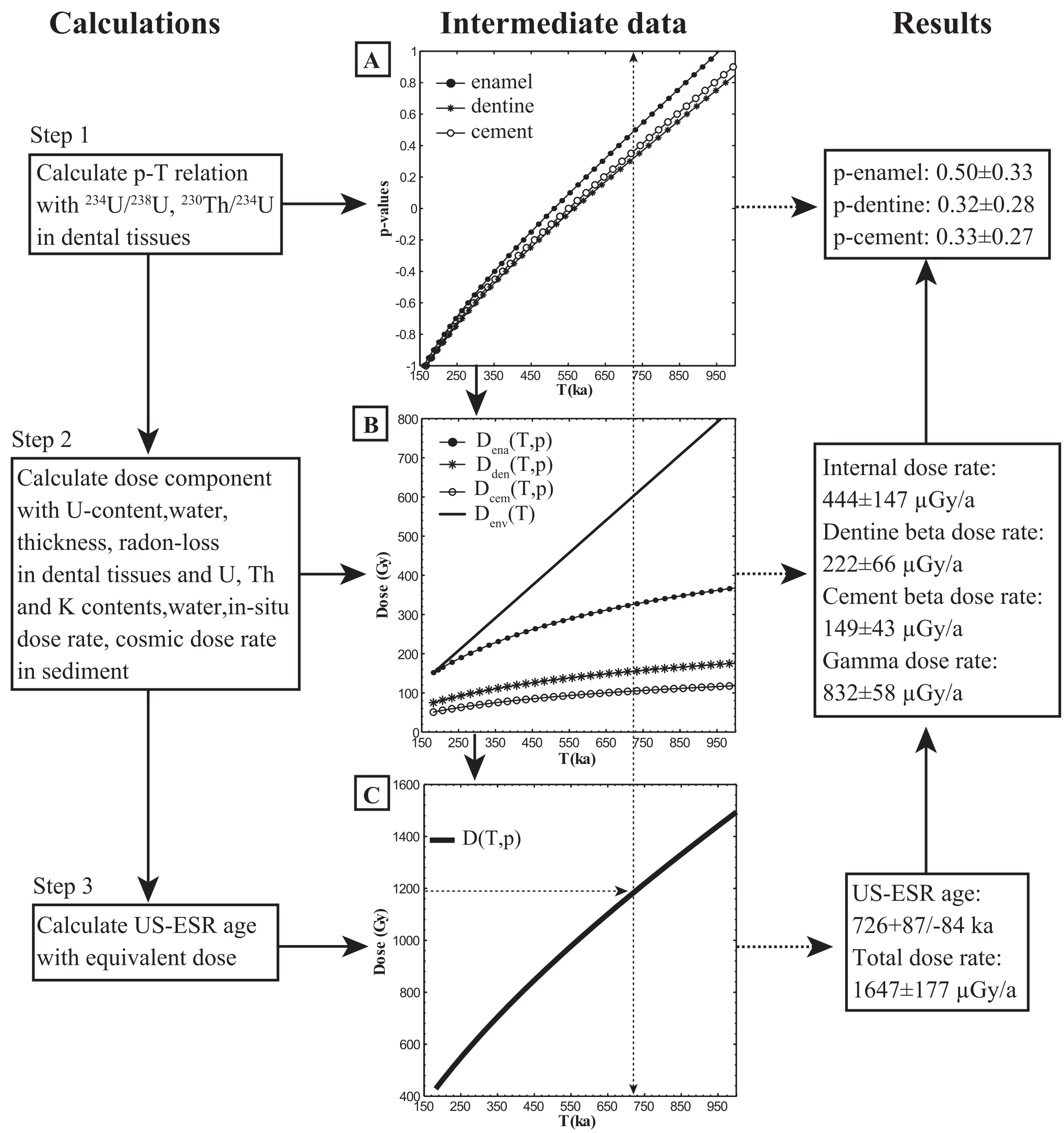

Fig. 1. An example illustrating the calculations of the US-ESR age, associated dose rates and U-uptake parameters.

specifics of U-uptake assumptions.

Acknowledgments

We gratefully thank Prof. Henry P. Schwarcz, McMaster University, for his thoughtful advice in setting up this research. The authors thank N. McLean and an anonymous reviewer, who provided insightful comments on this paper. Q.S. thanks the Erasmus Mundus program and the MNHN for providing scholarship for this study.

Appendix 1. Solving for the concentrations

With the approximations made in Section 2, Eq. (12) is obtained:

$$U_8(t) = U_{8m}(t/T)^{p+1}. \tag{A1}$$

Inserting $U_8(\tau) = U_8(t)\,(\tau/t)^{p+1}$ into Eq. (7), and from Eq. (11) follows:

$$S_4(\tau) = \frac{\lambda_8 r_0}{\lambda_4} U_8(t)(p+1)\tau^p \Big/ t^{p+1} \tag{A2}$$

And Eq. (13) can be expressed as:

$$U_4(t) = \frac{\lambda_8}{\lambda_4} U_8(t) \int_0^t \left[\lambda_4(\tau/t)^{p+1} + r_0(p+1)\tau^p \Big/ t^{p+1}\right] e^{-\lambda_4(t-\tau)} d\tau. \tag{A3}$$

Using $s = \tau/t$ yields:

$$U_4(t) = \frac{\lambda_8}{\lambda_4} U_8(t) \int_0^t \left[(\lambda_4 t)s^{p+1} + r_0(p+1)s^p\right] e^{-\lambda_4 t(1-s)} ds. \tag{A4}$$

An integration by parts allows the second integral to be written as:

$$\int_0^1 (p+1)s^p e^{-\lambda_4 t(1-s)} ds = 1 - \lambda_4 t \int_0^1 s^{p+1} e^{-\lambda_4 t(1-s)} ds \tag{A5}$$

and Eq. (A4) becomes:

$$U_4(t) = \frac{\lambda_8}{\lambda_4} U_8(t) \left[r_0 + \lambda_4 t(1-r_0) \int_0^1 s^{p+1} e^{-\lambda_4 t(1-s)} ds\right] \tag{A6}$$

which is Eq. (13) of Section 2.

For $U_0(t)$, an integration by parts in Eq. (8) gives:

$$\begin{aligned} U_0(t) &= \frac{\lambda_4}{\lambda_0}\left[U_4(t) - \int_0^t U_4'(\tau) e^{-\lambda_0(t-\tau)} d\tau\right] \\ &= \frac{\lambda_4}{\lambda_0}\left[U_4(t) - \int_0^t (S_4(\tau) + \lambda_8 U_8(\tau) - \lambda_4 U_4(\tau)) e^{-\lambda_0(t-\tau)} d\tau\right] \end{aligned} \tag{A7}$$

using Eq. (2) in Eq. (A7). Thus

$$\begin{aligned} \lambda_0 U_0(t) = {} & \lambda_4\left[U_4(t) - \int_0^t (S_4(\tau) + \lambda_8 U_8(\tau)) e^{-\lambda_0(t-\tau)} d\tau\right] \\ & + \lambda_4 \int_0^t \lambda_4 U_4(\tau) e^{-\lambda_0(t-\tau)} d\tau. \end{aligned} \tag{A8}$$

Eq. (8) shows that the last integral is $U_0(t)$, which results in:

$$(\lambda_0 - \lambda_4) U_0(t) = \lambda_4\left[U_4(t) - \int_0^t (S_4(\tau) + \lambda_8 U_8(\tau)) e^{-\lambda_0(t-\tau)} d\tau\right]. \tag{A9}$$

As above in Eq. (A3), introducing $s = \tau/t$ results in:

$$\begin{aligned} & \frac{\lambda_8}{\lambda_4} U_8(t) \int_0^1 \left[(\lambda_4 t)s^{p+1} + r_0(p+1)s^p\right] e^{-\lambda_0 t(1-s)} ds \\ & = \frac{\lambda_8}{\lambda_4} U_8(t) \left[r_0 + (\lambda_4 - r_0\lambda_0)t \int_0^1 s^{p+1} e^{-\lambda_0 t(1-s)} ds\right] \end{aligned} \tag{A10}$$

with the same integration by parts as above. Substituting from (A6) for $U_4(t)$ yields:

$$\begin{aligned} U_0(t) = \frac{\lambda_8 U_8(t)}{\lambda_0 - \lambda_4}\Bigg[& \lambda_4 t(1-r_0) \int_0^1 s^{p+1} e^{-\lambda_4 t(1-s)} ds - (\lambda_4 \\ & - r_0\lambda_0)t \int_0^1 s^{p+1} e^{-\lambda_0 t(1-s)} ds \Bigg] \end{aligned} \tag{A11}$$

which is the expression in Eq. (14).

Appendix 2. Derivation of the *p*–*T* relationship

For notational convenience we write:

$$I_0 = I_0(p,T) = \lambda_0 T \int_0^1 s^{p+1} e^{-\lambda_0 T(1-s)} ds \tag{A12}$$

and similarly for I_4. The Eq. (15) can be written as:

$$R_{48}(T) = r_0 - (r_0 - 1) I_4 \tag{A13}$$

yielding:

$$r_0 = (R_{48}(T) - I_4)/(1 - I_4). \tag{A14}$$

Also, Eq. (16) is:

$$\begin{aligned} R_{08}(T) &= \frac{\lambda_0}{\lambda_0 - \lambda_4}\left[-(r_0 - 1)I_4 - \left(\frac{\lambda_4}{\lambda_0} - r_0\right) I_0\right] \\ &= \frac{\lambda_0}{\lambda_0 - \lambda_4}\left[R_{48}(T) - r_0 - \left(\frac{\lambda_4}{\lambda_0} - r_0\right) I_0\right] \end{aligned} \tag{A15}$$

using (A13). Solving for r_0 in (A15) gives:

$$r_0 = \left[R_{48}(T) - \left(\frac{\lambda_0 - \lambda_4}{\lambda_0}\right) R_{08}(T) - \frac{\lambda_4}{\lambda_0} I_0\right] \Big/ (1 - I_0). \tag{A16}$$

Eqs. (A14) and (A16) then directly lead into the Eq. (19) in the main text.

Appendix 3. Calculating the total dose

Eq. (21) defines:

$$D_{ena}(T,p) = \int_0^T \left[C_8 U_8(t) + \frac{\lambda_4}{\lambda_8} C_4 U_4(t) + \frac{\lambda_0}{\lambda_8} C_0 U_0(t)\right] dt. \tag{A17}$$

Considering each of the terms separately and using the solutions in Eqs. (12)–(14) one has:

$$C_8 \int_0^T U_8(t) dt = \frac{C_8 U_{8m}}{T^{p+1}} \int_0^T t^{p+1} dt = \frac{C_8 U_{8m} T}{p+2}. \tag{A18}$$

After carrying out the integral using Eqs. (12) and (13)

$$\frac{\lambda_4}{\lambda_8}C_4\int_0^T U_4(t)dt = r_0\frac{C_4U_{8m}T}{p+2} - \lambda_4(r_0-1)C_4$$
$$\int_0^T U_8(t)t\left(\int_0^1 s^{p+1}e^{-\lambda_4 t(1-s)}ds\right)dt = r_0\frac{C_4U_{8m}T}{p+2}$$
$$-C_4\frac{U_{8m}\lambda_4}{T^{p+1}}(r_0-1)\int_0^T t^{p+2}\left(\int_0^1 s^{p+1}e^{-\lambda_4 t(1-s)}ds\right)dt. \quad \text{(A19)}$$

Similarly, using Eqs. (12) and (14) as above

$$\frac{\lambda_0}{\lambda_8}C_0\int_0^T U_0(t)dt = \frac{\lambda_0}{\lambda_0-\lambda_4}C_0\left[\begin{array}{l}(r_0\lambda_0-\lambda_4)\int_0^T U_8(t)t\left(\int_0^1 s^{p+1}e^{-\lambda_0 t(1-s)}ds\right)dt \\ -\lambda_4(r_0-1)\int_0^T U_8(t)t\left(\int_0^1 s^{p+1}e^{-\lambda_4 t(1-s)}ds\right)dt\end{array}\right]. \quad \text{(A20)}$$

Making the change of variables $u = t/T$ in the iterated integrals, adding and grouping terms results in the Eq. (23) for $D_{ena}(p,T)$. The other terms are obtained by following the same procedure.

Appendix 4. Numerical schemes

4.1. Computing the p−T relationship

For a given $p \geq -1$ the function in Eq. (19) can be solved numerically for $x(=\lambda_0 T)$ using Matlab with the integral appearing in Eq. (20) calculated using the trapezoidal approximation. For $R_{48} = 1.37$; $R_{04} = 0.81$ and $c = \lambda_4/\lambda_0 = 0.308$ the Matlab code is:

```
% relation_ new.m
function [result] = relation_ new(x, p)
ds =0.000001;
s = ds : ds : 1;
result = zeros(size(x));
for i = 1 : length(result)
    result(i) = 0.37./(1-0.308.* x(i).* exp(-0.308.* x(i)).* trapz(s, s.^(p
+1).* exp(0.308.*x(i).* s)))-0.294./(1- x(i).*exp(-x(i)).*trapz(s,
s.^(p+1).*exp(x(i).*s)))+0.692;
end

% relation_caller.m
p = -1:0.05:1;
x0 = 1;
root = zeros(size(p));
for i = 1 : length(p)
    root(i) = fsolve(@(x)relation_new(x, p(i)), x0);
end
root;
```

Using the plot function in Matlab:
plot (root/λ_0, p)
results in the graph in Fig. 1A. While the graph appears almost linear, it is possible to obtain a functional relation of the form

$$x(p) = x(-1) + b(p+1)^a. \quad \text{(A21)}$$

This can be accomplished by taking the natural log of Eq. (A19) in the form:

$$ln(x(p) - x(-1)) = a\,ln(p+1) + lnb \quad \text{(A22)}$$

and doing a linear fit of the data ($x(p_i) = x(i)$ listed above) in ($x(p_i) - x(1)$) vs $p_i + 1$ for $i = 2, \ldots, n$. The Matlab code for this is:

```
% relation_fit.m
p_new = p(2:end);
root_new = root(2:end);
X = log(p_new+1);
for i = 1:length(root_new)
    y(i) = log(root_new(i) - root(1));
end
mdl = fitlm(X, y);
beta0 = mdl.Coefficients.Estimate(1, 1);
beta1 = mdl.Coefficients.Estimate(2, 1);
coefficient = exp(beta0)
exponent = beta1
```

4.2. Computing the total dose

At each step of the procedure outlined in Section 5, a value of p_i and the corresponding $x_i = (\lambda_0 T_i)$ are given and one must calculate the corresponding total dose $D(p_i, T_i)$ for comparison with the measured total dose, D_e. This is a straightforward calculation in

Matlab with the single and double integrals that appear calculated numerically using the functions.

The Matlab code for calculating the integrated dose components of, D_{ena} (T, p), D_{den} (T, p), and D_{cem} (T, p) is:

```
% Newton-Raphson iterative scheme and Simpson rule
function [DE]=NRS(T, p, r0, U8, C8, C4, C0)
    DC=[2.8263, 9.1577]*10^(-3);
    c=DC(1)/DC(2); k=1-c;
    p=p+1;
    N=length(T);M=N;
    t=[0.25,0.5,0.75];
    for k=1:N;
        for L=1:3
            fun1=@(x, y) (x^p(k)-t(L)*T(k)*DC(1)*y);
            [A, B]=ode45(fun1,[0 1], 0);
            RK1=B(length(B));
            fun2=@(x, y) (x^p(k)-t(L)*T(k)*DC(2)*y);
            [A, B]=ode45(fun2,[0 1], 0);
            RK2=B(length(B));
            Y(1,L)=t(L)^(p(k)+1)*RK1;
            Y(2,L)=t(L)^(p(k)+1)*RK2;
        end
        y1=@(t)t.^p(k).*exp(-DC(1)*T(k)*(1-t));I=double(quad(y1,0,1));
        y2=@(t)t.^p(k).*exp(-DC(2)*T(k)*(1-t));J=double(quad(y2,0,1));
        Yt(1,k)=0.25/3*(4*(Y(1,1)+Y(1,3))+2*Y(1,2)+I);
        Yt(2,k)=0.25/3*(4*(Y(2,1)+Y(2,3))+2*Y(2,2)+J);
        if isnan(Yt(1,k))==1
            M=k-1;
            Yt(:, k)=[];
             break
        elseif isnan(Yt(2,k))==1
            M=k-1;
            Yt(:, k)=[];

            break
        end
    end
    YT4=Yt(1,:);YT0=Yt(2,:);
    F1=U8*(C8+C4.*r0)./(p+2);
    F2=U8*C4*DC(1).*T.*(r0-1).*YT4;
    F3=U8*C0*DC(2)./(DC(2)-DC(1)).*T.*(((r0*DC(2)-DC(1)).*YT0-DC(1)*(r0-
1).*YT4));
    DE=(F1-F2+F3).*T;
```

References

Cheng, H., Edwards, R.L., Shen, C.-C., Polyak, V.J., Asmerom, Y., Woodhead, J., Hellstrom, J., Wang, Y., Kong, X., Spötl, C., Wang, X., Alexander, E.C., 2013. Improvements in ^{230}Th dating, ^{230}Th and ^{234}U half-life values, and U-Th isotopic measurements by multi-collector inductively coupled plasma mass spectrometry. Earth Planet. Sci. Lett. 371–372, 82–91.

Grün, R., 1994. A cautionary note: use of ‘water content’ and ‘depth for cosmic dose rate’ in the AGE and DATA programs. Anc. TL 12, 50–51.

Grün, R., 2000. An alternative model for open system U-series/ESR age calculations: (closed system U-series)-ESR, CSUS-ESR. Anc. TL 18, 1–4.

Grün, R., 2009. The DATA program for the calculation of ESR age estimates on tooth enamel. Quat. Geochronol. 4 (3), 231–232.

Grün, R., Eggins, S., Kinsley, L., Mosely, H., Sambridge, M., 2014. Laser ablation U-series analysis of fossil bones and teeth. Palaeogeogr. Palaeoclimatol. Palaeoecol. 416, 150–167.

Grün, R., Katzenberger-Apel, O., 1994. An alpha irradiator for ESR dating. Anc. TL 12, 35–38.

Grün, R., Schwarcz, H.P., Chadam, J., 1988. ESR dating of tooth enamel: coupled correction for U-uptake and U-series disequilibrium. Nucl. Tracks Radiat. Meas. 14, 237–241.

Guérin, G., Mercier, N., Adamiec, G., 2011. Dose-rate conversion factors: update. Anc. TL 29, 5–8.

Marsh, R.E., 1999. Beta-gradient Isochrons Using Electron Paramagnetic Resonance: Towards a New Dating Method in Archaeology (M.Sc. thesis). McMaster University, Hamilton.

Nathan, R., Grün, R., 2003. Gamma dosing and shielding of a human tooth by a mandible and skull cap: Monte Carlo simulations and implications for the accuracy of ESR dating of tooth enamel. Anc. TL 21, 79–84.

Prescott, J.R., Hutton, J.T., 1994. Cosmic ray contributions to dose rates for luminescence and ESR dating: large depths and long-term time variations. Radiat. Meas. 23, 497–500.

Shao, Q., Bahain, J.-J., Dolo, J.-M., Falguères, C., 2014. Monte Carlo simulation of US-ESR age uncertainty. Quat. Geochronol. 22, 99–106.